

THE DEVELOPMENT OF A EUROPEAN HELICOPTER NOISE MODEL

Marthijn Tuinstra, marthijn.tuinstra@nlr.nl, NLR – Netherlands Aerospace Centre (Netherlands)

Nico van Oosten, Anotec Engineering (Spain)

Herold Olsen, SINTEF (Norway)

Abstract

No international consensus yet exists on a method for helicopter noise contour calculation for land-use planning. An intermediate approach is recommended in the Environmental Noise Directive (END) to model helicopters in a similar manner as fixed-wing aircraft. This method however, lacks the capability to capture the complex nature of helicopter noise adequately. The European Commission commissioned the development a helicopter noise model to be part of a public European environmental model suite for aviation. A helicopter noise calculation method was defined based on the current state-of-the-art, which was subsequently implemented in a software prototype (NORAH). Through dedicated flight test campaigns noise hemispheres were established for eight helicopter types, covering the noise relevant regions of the flight envelope. Based on these noise databases the noise emission of 70% of the helicopters flying in Europe can be represented in the NORAH model.

1. INTRODUCTION

Helicopter noise emission is strongly dependent on flight conditions and varies heavily with emission angle. Currently used land-use-planning methods in Europe developed for fixed wing aircraft (ECAC Doc 29¹) are recognized not to be able to represent helicopter noise with sufficient fidelity. The European Commission therefore commissioned the development of a European approach to helicopter noise modelling. The work comprised the definition of a method², the acquisition of helicopter noise databases^{3,4} to feed the model with empirical data and the development of a software prototype⁵. The modelling approach follows closely that of the Helicopter Environmental Noise Analysis tool (HELENA), which represents the state-of-the-art of helicopter noise modelling in Europe. A second source of reference is a recent study⁶ commissioned by National Academies of Science Airport Cooperative Research Program, which lead to a set of recommended key community noise modelling elements that are

required to accurately predict helicopter sound. This paper aims at providing an overview of the newly established European helicopter noise model and concludes with recommendations for future developments.

2. HELICOPTER NOISE MODELLING

2.1. Fleet model

To be useable for land-use-planning it is required that the model is able to represent the bulk of the European helicopter fleet. In today's fleet, there are over 350 different helicopter types: too many to perform individual noise measurements. The helicopter fleet modelling aims at identifying those helicopters that aggregately represent 70% of the helicopter noise nuisances, therefore enabling the development of a representative noise model based on just a limited set of helicopter classes.

For this purpose, a survey of civil helicopters in Europe was prepared. From the circa 7400 helicopter registrations by the end of 2014, about 350 different helicopter types and 92 ICAO aircraft type designators were derived. Subsequently, the predominant type of operation was added to each helicopter type, including data on the expected number of flight hours per helicopter per annum and average number of take-offs/landings per flight hour, and, wherever possible, helicopter configuration-related weight and noise data. Helicopter types with comparable type designator, configuration, weight and noise data were grouped together in approximately 50 helicopter classes.

Copyright Statement

The authors confirm that they, and/or their company or organization, hold copyright on all of the original material included in this paper. The authors also confirm that they have obtained permission, from the copyright holder of any third party material included in this paper, to publish it as part of their paper. The authors confirm that they give permission, or have obtained permission from the copyright holder of this paper, for the publication and distribution of this paper as part of the ERF proceedings or as individual offprints from the proceedings and for inclusion in a freely accessible web-based repository.

These helicopter classes were ranked by number of helicopters per class, total number of flight hours per class per year and total number of take-offs and landings per class per year. A selection of representative classes eligible for noise measurements, was finally made from the top-20 helicopter class ranking.

To ensure a coverage of >70% of the European helicopter fleet, eight helicopter classes were identified, represented by the helicopters types marked in red in table 1. Together, these helicopter classes represent approximately (see also figure 1):

- 72% of the total number of helicopters
- 69% of the total number of flight hours per year
- 82% of the total number of take-offs/landings per year.

Table 1 List of helicopter classes, helicopter types between brackets are mirrored configurations

Helicopter class	ATD	Included helicopter types
AS350 Ecureuil	AS50	AS50, ALO2, ALO3, LAMA, PSW4
Bell 206 JetRanger	B06	B06, B06T, B47T, H12T, R66
Bell 412	B412	B412, B430, S76
EC120 Colibri	EC20	EC20, EC30, GAZL
EC135	EC35	EC35, EC145T2
Robinson 22	R22	R22, CH7, V500, [A600], [BABY], [DRAG], [EXEC], [SCOR], plus a number of homebuilts
Robinson 44	R44	R44, B47G, B47J, ELTO, UH12
Schweizer 300	H269	H269, BRB2, EN28, [ZA6]

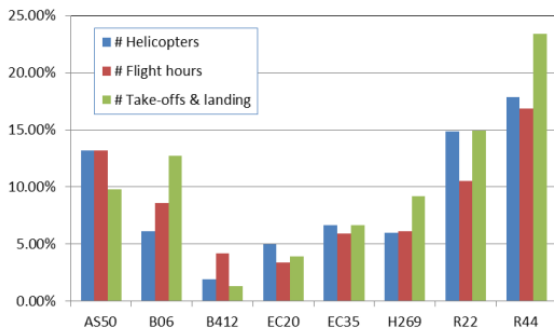


Figure 1 - Percentage of total number of helicopters, flight hours and Take-offs & landings

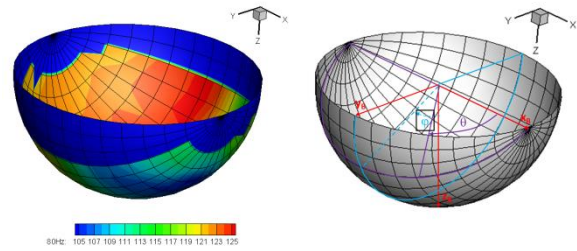


Figure 2 Example of a noise hemisphere (left), based on measurements of a R22 helicopter, 80Hz 1/3 octave band frequency, given in aircraft body axis system(right)

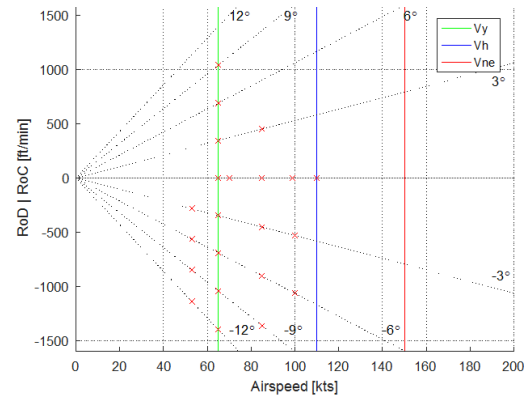


Figure 3 EC120 noise measurements points distribution in the flight envelope, in this Vy is the best rate of climb speed, Vh velocity for level flight at maximum continuous power and Vne the never to exceed velocity

2.2. Source model

A hemisphere approach was followed to describe the helicopter noise source. Next-generation helicopter noise models (HELENA⁷, AAM⁸ and SELENE⁹) all employ hemispheres (see figure 2), demonstrating a clear consensus on how to adequately capture the complex and highly directive nature of helicopter noise.

Hemisphere noise levels are defined at a fixed reference distance of 60m and include effects of atmospheric absorption under ICAO atmospheric reference conditions. Hemispheres are given in one-third octave bands, for frequencies between 10Hz (10th band) to 10 kHz (40th band). Hemispheres are defined as function of azimuth φ and polar angle θ , binned in intervals of 10 degrees.

For a complete helicopter noise source characterisation a set of hemispheres is needed that covers the entire range of relevant air speeds and flight angles within the flight envelope. Figure 1 in Gervais et al.⁷ shows that due to the occurrence of Blade Vortex Interaction the strongest variation of noise levels is found for descent angles. Specific attention should



Figure 4 Helicopter types selected for noise measurements (top, left to right): Robinson R22 and R66, Eurocopter EC120 and EC135; (bottom) Robinson R44, Airbus Helicopters AS350, Bell B412 and Schweizer S300

therefore be given to this part of the flight envelope. An example of a noise measurement point distribution in the flight envelope of the EC120 is given in figure 3.

Since it not realistic to obtain noise databases for all 350 helicopter types in Europe a substitution method is employed. The premise is that when one would group helicopters of similar characteristics together into a single helicopter class, similar noise emission characteristics can be expected. To allow variations in noise levels within a class, and do justice to the efforts done by manufacturers to make their helicopter models as silent as possible, an offset of hemisphere levels based on the difference (ΔL_{EPNL}) between registered certification levels¹⁰ of the class reference and the helicopter type under consideration is applied. The noise level for a helicopter type in class i at flight condition j and emission angles φ and θ is then given by

$$(1) \quad L_{i,j}(f, \varphi, \theta) = \tilde{L}_h(f, \pm\varphi, \theta)_{i,j} + \Delta L_{EPNL}$$

in which \tilde{L}_h is the interpolated hemisphere noise level of the reference type. For helicopter types that are shown between brackets in table 1 the helicopter configuration is mirrored with respect to the reference and hence the azimuth angle needs to be reversed.

2.3. Propagation model

Unlike the Noise Power Distance relationships employed in ECAC Doc 29, the modelling of source and propagation is carried out independently. In order to predict the noise levels experienced by a person on the ground from the helicopter noise hemispheres, atmospheric propagation effects need to be accounted for. The noise levels are attenuated with increasing distance due to spherical spreading losses (ΔL_s), atmospheric attenuation (ΔL_a), ground attenuation and reflection (ΔL_g).

$$(2) \quad \Delta L_p = \Delta L_s + \Delta L_a + \Delta L_g$$

To account for these effects, established public noise models^{11,12,13} are used. Equations (1) and (2) together yield the noise levels at an observer position.

$$(3) \quad L_o(f, t) = L_{i,j}(f, \varphi, \theta) + \Delta L_p(f, \mathbf{x}, \mathbf{y})$$

3. HELICOPTER NOISE DATABASES

3.1. Microphone measurements

To ensure the highest data quality, where applicable, the noise measurements were performed according the guidelines and restrictions as outlined in ICAO Annex 16, Chapter 8¹⁴.

Eight helicopter types were rented from helicopter operators for the noise measurements. These included the R22, R44 and R66 helicopter types, EC120 and EC135, AS350, B412 and S300 helicopter type (see figure 4). The noise measurements were performed at two test sites in the Netherlands (NLR-Flevoland and former airforce base Luitenant-Generaal Bestkazerne) and one test site in Spain (Marugan airfield).

A 420-metre-wide microphone line array comprising 17 microphones on 40cm diameter ground plates was used to perform the noise measurements (figure 5). The exact lateral distances are given in table 2. The setup allows for the detailed capturing of the directivity pattern for the emission angles that are relevant for noise nuisance evaluation. Additionally, 3 microphones were mounted on a tripod at 1.2m height at certification positions for data quality control purposes.

The recorded emission angles are defined as:

- Polar emission angles that occur within the 10dB-down time interval based on Sound Exposure Level (SEL)

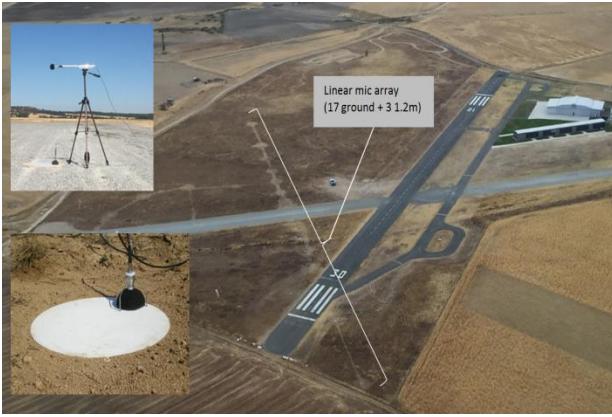


Figure 5 Test setup at Marugan airfield

Table 2 microphone lateral distances

y, m	0	10	25	40	62	87	115	150	210
------	---	----	----	----	----	----	-----	-----	-----

- Azimuthal (or lateral) emission angles +/- 60° from the vertical

Although it is desirable to measure lateral angles exceeding 60° this would have resulted in an exponential growth in complexity and cost of the measurements. The measurement of near parallel-to-surface propagating noise over long distances would have negatively affected data quality, therefore requiring a complex experimental setup with vertical arrays^{15,16}. In general, the added cost cannot be justified set against the added-value.

1/3 Octave band spectra were acquired with a 0.1s interval for a 10Hz to 10kHz frequency range. A central ground station consisting of a mobile office on which a 10m mast with weather station was mounted, was used to measured temperature, relative humidity, barometric pressure, wind speed and direction. Measurements were automatically stored on a PC and actual weather conditions continuously checked against applicable ICAO limits.

3.2. On-board measurements

A novel carry-on flight data recorder (COFDR) was developed and used to instrument the rented helicopters. The helicopter trajectories were synchronically measured with the noise measurements by differential GPS. To acquire live data from the helicopter instrument panel an NLR in-house developed^{3,4} on-board video data acquisition system with real-time image processing was employed, recording relevant meta-data such as velocity of the helicopter and rotor RPM. All tests were performed at 90% MTOW or higher. The COFDR individual components and functions are listed in table 3 and shown in figure 5.

Table 3 Components of the COFDR

Component	Description
GNSS receiver & antenna	Measures position, time and velocity
Inertial Measurement Unit (IMU)	Measures roll and pitch attitude, and roll, pitch and yaw angular rates, and helicopter acceleration in x/y/z
SmartCam	Measured indicated air speed (IAS), rotor rpm (RPM), vertical speed (VS) and altitude (ALT) indicators
tachometer	Measures main rotor RPM
Laptop	Records measured parameters and provides pilot guidance

The flight data was acquired and processed by the carry-on system in real-time and sent to a guidance application, (ANOTEC's pilot guidance unit). This unit supported the flight test engineer and the pilot to correctly perform the flight tests within the procedural margins). Imagery and data is also recorded for post-flight analysis.

A single helicopter noise measurement campaign consisted of a two-day programme with 4-5 hours of effective measurements per day. The measurements covered ICAO Annex 16 reference procedures and, in addition, "real-life operating" procedures and flight conditions (see figure 3). In total, the combined helicopter noise measurement campaigns covered more than 170 test conditions, 800 runs and 60 flight hours,

3.3. Hemisphere processing

Figure 7 shows the parameters and definitions required for hemisphere processing.

For a particular time instance, the helicopter was positioned at $\mathbf{x}_h (x_h, y_h, z_h)$, where \mathbf{x}_h is defined in the local coordinate system $x-y-z$. The $x_B-y_B-z_B$ axis of the helicopter body axis system ($x_B-y_B-z_B$) was assumed to be aligned in local coordinate system x -axis (helicopter attitude is not considered). The positive y_B and z_B -axis were directed to the right of the helicopter and downwards respectively.

Hemispheres require both helicopter position data and noise data as a function of time. One-third Octave band spectra were stored every 0.1s, providing the band levels as function of recorded time, frequency and microphone position

$$(4) \quad L = L(t_r, f, \mathbf{x}_m^i)$$



Figure 6 Carry-On Flight Data Recorder (COFDR): SmartCam digitization of performance indicators (top left); camera mounting (top right); Laptop, GNSS receiver and IMU (bottom left), EC120 instrument panel and optical tachometer (bottom right)

The helicopter dGPS measured position was stored every 0.2s being a function of emission time:

$$(5) \quad \mathbf{x}_h = \mathbf{x}_h(t_e)$$

Recorded time and emission time were related to each other by the distance between helicopter and microphone and the speed of sound:

$$(6) \quad t_r = t_e + \frac{r}{c}$$

where c is the speed of sound. Equation (6) allows expressing the helicopter position as function of recorded time for a given microphone. By linear interpolation the helicopter position can then be estimated for a given recorded time.

Prior to the hemisphere generation process, the noise measurement data were corrected and scaled to hemisphere reference conditions at each time instance. This involves the steps outlined in figure 8. In the first step corrections are applied to raw measured 1/3 octave bands for cable length, microphone frequency response, free field and windscreen corrections.

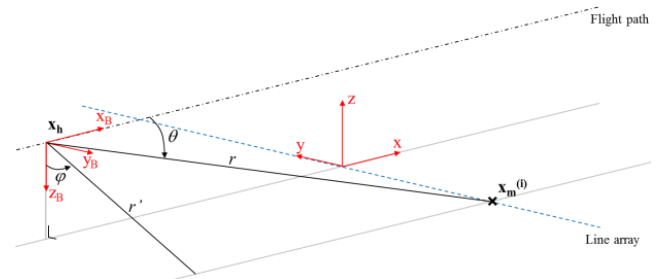


Figure 7: Axis and observer angle definition

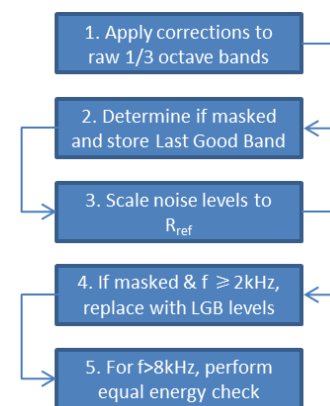


Figure 8 Flow chart preprocessing of noise data

Secondly, for each recorded spectrum the Last Good Band¹⁴ (LGB, 3dB above background noise levels) is determined. Subsequently, the noise levels are scaled to a reference distance r_h of 60m by multiplication of the noise powers by a scale factor

$$(7) \quad S(f) = 10^{\frac{\alpha(f)r - \alpha_h(f)r_h}{10}} \cdot \left(\frac{r}{r_h}\right)^2$$

in which α and α_h are the atmospheric attenuation in dB/m, calculated according to SAE ARP 5534¹¹, at measurement and reference atmospheric conditions respectively. In the fourth step, masked bands are replaced by the LGB noise levels. Finally, an *equal energy check* is performed for unmasked scaled noise levels above 8kHz. In case the scaled noise levels increase more than 3dB in the next one-third octave band, the following band levels are replaced by the current band level. The rationale is that there is no physical reason for noise levels increasing strongly at the highest frequencies. Failing to detect the LGB due to a temporary increase in background noise levels or linear scaling of non-linear propagated noise may lead to extreme high but non-physical scaled high frequency noise levels. Based on the corrected and scaled noise powers the hemispheres are derived. An example of a pre-processed run is provided in figure 11.

Two conceptual hemispheres E and W are defined containing the summed acoustic energy and fractional number samples per hemisphere bin. For a flown procedure, all recorded one-third octave bands within the 10-dB down time will fill the hemisphere, as shown schematically in figure 9.

By eq. (6) the helicopter position at recorded time t_r is found. The polar angle θ , azimuth angle φ and distance r is calculated for each microphone. The four nearest bins are identified and a weight factor, inversely proportional with the distance to the bin centre, is calculated according to

$$(8) \quad w_{m,n} = \left(1 - \frac{|\varphi - \varphi_m|}{\Delta\varphi}\right) \left(1 - \frac{|\theta - \theta_n|}{\Delta\theta}\right)$$

In this m and n are the azimuth and polar bin index respectively (see figure 10) and $\Delta\varphi = \Delta\theta = 10^\circ$ is the hemisphere resolution. The hemisphere W is updated by summation of the newly calculated weights to the affected bins. Subsequently, the increment of acoustic energy is calculated by

$$(9) \quad \Delta E_{m,n} = w_{m,n} \cdot 10^{\frac{L(f,\varphi,\theta)}{10}}$$

, where L' is the corrected and scaled noise level. The hemisphere E is updated by summation of $\Delta E_{m,n}$ to the affected bins.

After processing all repeat runs the hemispheres representing a single flight condition are ready to be merged into a single hemisphere. To ensure high quality of the noise data it is demanded that 90% of the acquired velocity samples are within ± 5 kts of the nominal velocity and that 90% of the acquired position samples located within the airspace contained between $\gamma \pm \gamma/12$ degrees (see figure 12). Runs not passing these checks are rejected. Finally, the merged hemisphere, in decibels per one-third octave band, is given by:

$$(10) \quad L_n = 10 \log_{10} \left[\frac{\sum_{i=1}^K E_i}{\sum_{i=1}^K W_i} \right] - \Delta G$$

where ΔG is the correction for the pressure doubling that occurs on the surface on the ground plate and K the number of valid repeat runs.

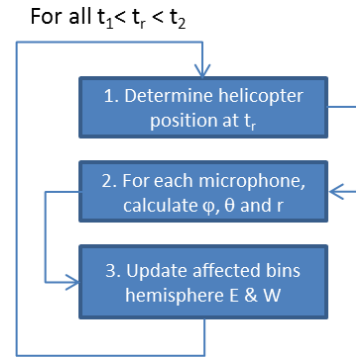


Figure 9 Flow chart hemisphere processing

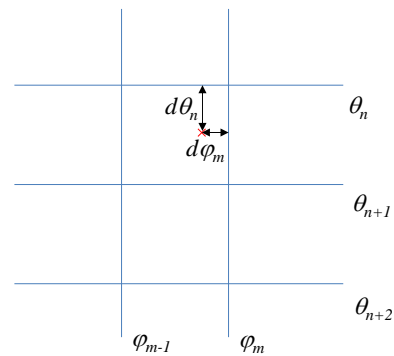


Figure 10: Interpolation stencil, the red cross indicates a measured φ and

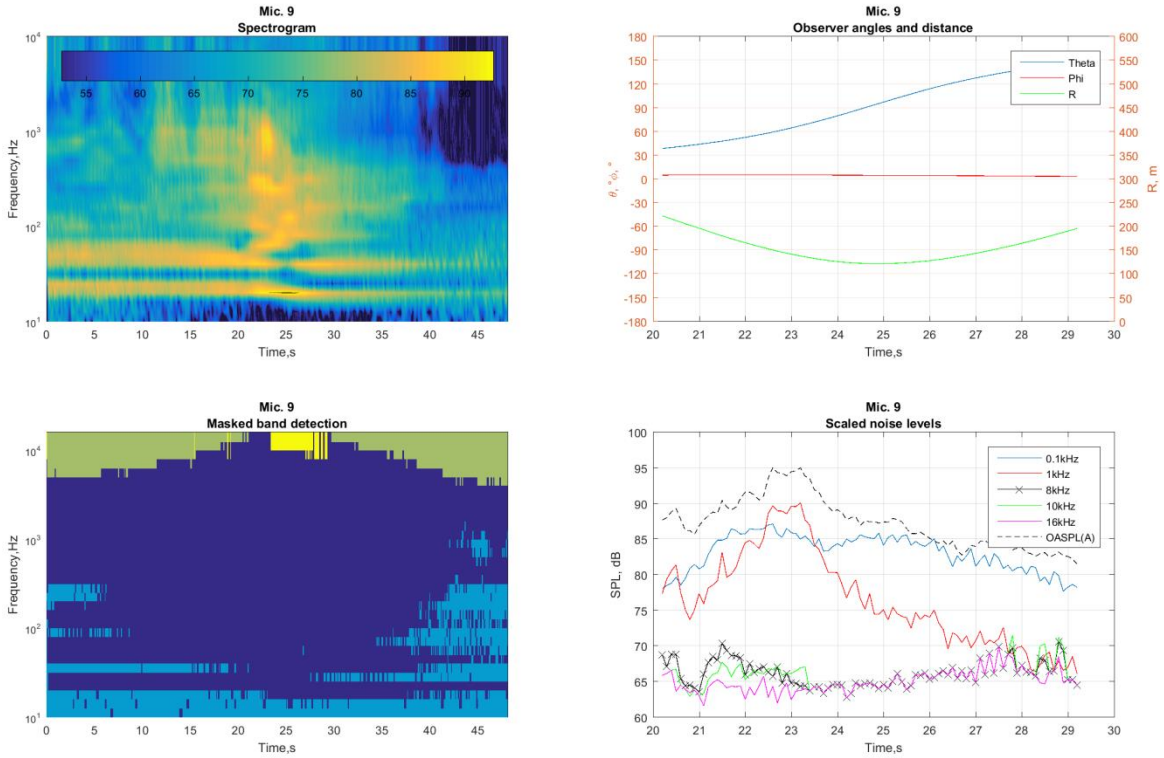


Figure 11: top left: spectrogram 1/3 octave band spectra every 0.1s, top right: Polar angle (theta), azimuth angle (phi) and distance from helicopter to microphone (R), bottom left: Masked band detection, (dark blue = 3dB>background noise, light blue = masked and uncorrected, green = masked and reconstructed, yellow = not masked, equal energy correction), bottom right : scaled noise levels for several 1/3 octave band frequencies & A-weighted OASPL

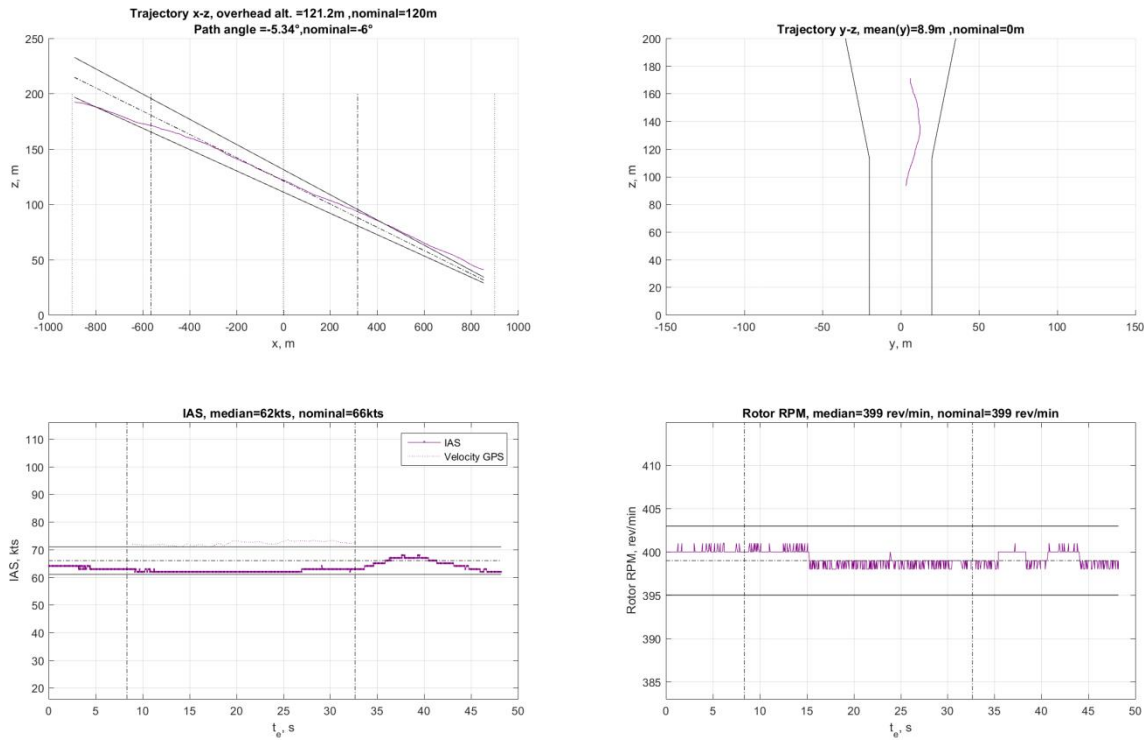


Figure 12: Helicopter position, Indicated Air Speed (IAS) and rotor RPM, 10dB down period is indicated by the dash-dotted vertical lines

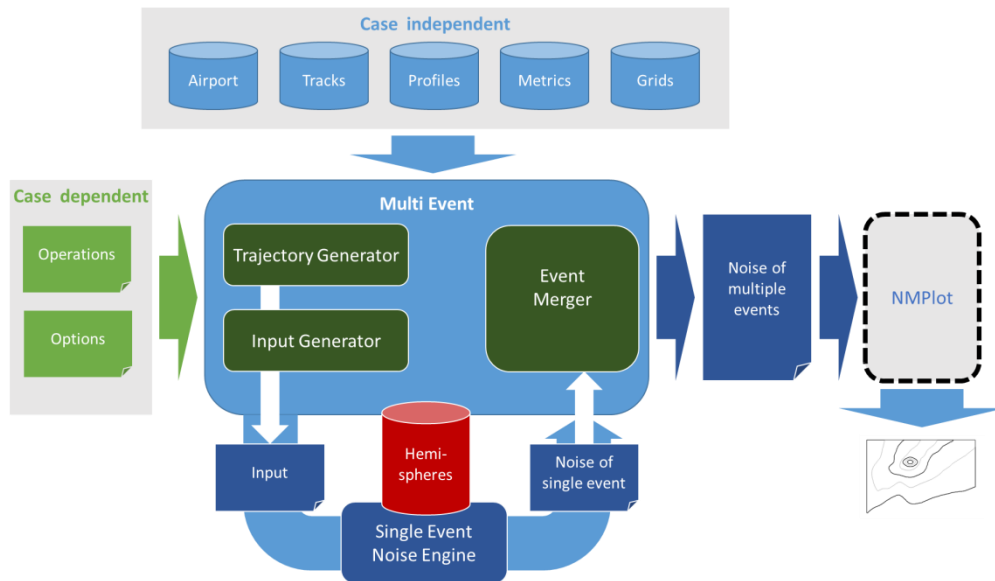


Figure 13 High level design of software prototype NORAH

4. SOFTWARE PROTOTYPE, NORAH

In section 2 a method is presented in which the NOise of Rotorcraft (is) Assessed by a Hemisphere-approach (NORAH). A software prototype⁵ for assessment of helicopter noise around airport was developed for implementing the proposed method - based on the high- level design given in figure 10. The following main elements have been defined as the core of the software prototype.

The *Single Event Module* is the main noise calculation engine and contains all processes needed to calculate the noise at an observer grid for a single helicopter flying a given 4D trajectory in accordance with the method described in section 2.

The *Multi Event Module* is a shell around the Single Event Module. Based on the user defined input it triggers this latter Module for each individual operation and captures the output for subsequent merging so as to calculate and output the total noise at the observers' position.

This core is fed with all required input data through plain text files that can easily be created with any text editor. Three levels of input exist:

Fixed input files shall not be edited by the user. This mainly concerns the database with hemispheres

Case independent input files shall be defined by the user, however only once for a study. This input can be seen as a database containing all (user-definable) parameters that may occur for the various scenarios within the study

In the *Case dependent input* files the user can build a specific scenario ("case") by selecting the relevant values for the different parameters from the case independent databases and in addition shall provide calculation options.

The output of the core will be a data file containing the final noise levels received at the required observer positions.

In order to facilitate future integration and also to maximize performance, both core modules (Single-Event and Multi-Event) were implemented in FORTRAN 95 and Python respectively, with ASCII interfaces that can easily be generated by and read from programming languages like C/C++, Python, Matlab, VB.net, C# and FORTRAN. Whilst the development of a GUI was outside the scope of the project, such a facility can easily be added. The software consists in two console programs (NORAH.exe and SingleEvt.exe) that operate in a three level folder structure (Airport, Case and Single Event level). At airport level, helipads, tracks, profiles and noise metrics are defined by means of ASCII tables with fixed names. Whilst noise metrics and profiles usually are common to most airports they are defined here to provide increased flexibility to the user. At Case level, airport operations and run options are defined. At Single event level, the noise levels calculated for each operation defined in the case are stored. For easy inspection of the calculation results the tool supports "nmplot" output format.

5. CONCLUSIONS AND RECOMMENDATIONS

5.1. Conclusions

A new helicopter noise modelling method is defined based on which, a software prototype was developed. A noise database was acquired allowing modelling of those helicopters responsible for more than 70% of the noise hindrance caused by the European helicopter fleet. The model is future-oriented, and can be enhanced according to future needs and knowledge development. The model differs from existing NPD-based methods for aircraft noise, like ECAC Doc 29, by separately handling the modelling of source and propagation. The spectral resolution of one-third octave bands is higher than required for END noise mappings; however, it answers to other demands related to optimized mitigation, sound proofing, auralization etc. The provision of source data below 50 Hz is well suited for future modelling of infrasound or blade-pass-frequency issues. Looking from a broader perspective, the new modelling method shows a way forward to a long awaited new direction within aircraft noise mapping that can overcome the limitations of single-number noise-power-distance characterizations inherited from the 1980s.

5.2. Recommendations

To improve the user experience and match the needs for land-use-planning extensive testing of NORAH amongst its potential user-base is recommended. Feedback should be collected on functionality and missing features, which will allow the evolution of the prototype into a full-fledged product. A set of recommendations on how to further improve the helicopter noise model itself follows below.

The base premise behind the helicopter fleet model that helicopters types of similar characteristics possess comparable noise characteristics should be further validated. This can be achieved by comparing noise measurements for helicopter types that are within a single class. Towards this end dedicated noise measurements could be performed, allowing extension of the database as well. Alternatively, existing datasets, other than the ones already included in the NORAH noise database, can be employed.

The A109 class should be considered first when extending the NORAH noise database. Covering 8% of the number of helicopters and 6% of the flight hours and take-offs and landings in Europe, this class would have a high impact on the aggregate percentage of helicopters that could be represented by the NORAH model.

To broaden range of helicopter weight classes represented in the model, the noise database should be extended by inclusion of heavy helicopter types – notably of the A139, S92 and AS32 class.

Hemispheres are derived for helicopters in steady flight conditions, considering various velocities and climb/descent angles. Further research into the relevance of noise hindrance due to transition between steady flight conditions, accelerated/decelerated flight segments, turns and hover is recommended in order to improve the model's fidelity.

The software prototype allows selecting velocities and path angles for which hemispheres are available. Although a broad range of hemispheres and related flight parameters are included, this is a limitation when compared to fixed-wing aircraft noise models like ECAC Doc 29. To increase the flexibility of defining flight trajectories interpolation between hemisphere conditions should be allowed.

For the present method the lowest considered frequency was reduced from 50Hz to 10Hz in order to capture the main rotor Blade Passage Frequency (BPF). The characteristic low frequency thumping noise of helicopters is known to cause hindrance, which is however not captured in any existing noise metric. The study of low frequency noise hindrance due to helicopters and development of a suitable noise metric is therefore recommended.

Finally, the propagation module should be further extended to include shielding effects, for example due to noise barriers, buildings, mountains, and other geometries in order to further increase the fidelity of the predictions.

ACKNOWLEDGEMENT

This work has been funded under the European Commission Service contract No. MOVE/C2/SER/2014-269/SI2.706115 for the development of a Public European Environmental Model Suite for Aviation.

REFERENCES

- [1.] ECAC, 'Report on Standard Method of Computing Noise Contours around Civil Airports', ECAC Doc29, 4th Ed., 2016
- [2.] M. Tuinstra, J. Stevens, N. van Oosten and H. Olsen, 'Towards a European helicopter noise calculation method', 44th European Rotorcraft forum, ERF-2018-46, 2018
- [3.] B. Timmerman, M. Tuinstra, R.M. Uiterlinden, N. van Oosten and S.E. Ionescu, 'Live optical digitisation of flight instruments for flight guidance in helicopter noise measurements', 43rd European Rotorcraft Forum, ERF-2017-539, 2017
- [4.] R.M. Uiterlinden, B. Timmerman, M. Tuinstra, N. van Oosten and S.E. Ionescu, 'Camera based flight test instrumentation', 43rd European Rotorcraft Forum, ERF-2017-534, 2017
- [5.] N. van Oosten, L. Meliveo, M. Tuinstra, H. Olsen, 'The new EU helicopter noise model NORAH', 11th European Congress and Exposition on Noise Control Engineering, Euronoise, 2018
- [6.] J.A. Page, C.M. Hobbs, B. May, E. Boeker, H. Brouwer, C. Morrow, 'Guidance for helicopter community noise prediction', ACRP Project No. 02-44, 2015
- [7.] M. Gervais, V. Gareton, A. Dummel and R. Heger, 'Validation of EC130 and EC135 environmental impact assessment using HELENA', American helicopter soc., 66th annual forum, Phoenix, 2010
- [8.] J.A. Page, C. Wilmer, T. Schultz, K.J. Plotkin and J. Czech, 'Advanced Acoustic Model Technical Reference and User Manual', 2009
- [9.] F. Guntzer, P. Spiegel and M. Lummer, 'Genetic optimization of EC-135 noise abatement flight procedures using an aeroacoustic database', 35th European rotorcraft forum, 2009
- [10.] EASA Noise Type Certificates Rotorcraft, Issue 21; 26 June 2015; <https://easa.europa.eu/document-library/noise-type-certificates-approved-noise-levels>
- [11.] SAE, 'Application of pure-tone atmospheric absorption losses to one-third octave-band data', ARP5534, 2013 / SAE ARP5534 (2013); Application of pure-tone atmospheric absorption losses to one-third octave band data. SAE, 2013
- [12.] Chien & Soroka (1975), "Sound Propagation along an Impedance Plane", Journal of Sound and Vibration, 43(1), pp.9-20 / C.F. Chien and W.W. Soroka (1976), "Sound propagation along an impedance plane", J. Sound Vib., 43:9-20
- [13.] M.E. Delaney and E.N. Bazley (1970), "Acoustic properties of fibrous absorbent materials", Appl. Acoust., Vol. 3, pp.105-116
- [14.] ICAO Annex 16 to the Convention on International Civil Aviation, Environmental protection, Vol. I, Aircraft noise, sixth edition, 2011
- [15.] M. Tuinstra, P. Sijtsma, "Measurement of helicopter noise hemispheres utilizing a 100m vertical array", European Rotorcraft Forum 2012, Amsterdam, ERF-2012-019, 2012
- [16.] R.W. Browne; Munt, R.M.; Simpson, C.R.; Williams, T.; Prediction of Helicopter Noise Contours for Land Use Planning, AIAA Paper 2004-2811, Manchester, UK, 2004